Numerical Simulation of Rolling Up of Leading/Trailing-Edge Vortex Sheets for Slender Wings

Yin Xie-yuan,* Xia Nan,* and Deng Guo-hua*
University of Science and Technology of China, Anhui, Hefei, China

In present paper we compute the rolling up of leading/trailing-edge vortex sheets and their interaction for delta and double-delta wings, using a simple two-dimensional discrete vortex model. The numerical results show that a trailing-edge vortex, which has an opposite sign of circulation of the leading-edge vortices, can be rolled up for both delta and double-delta wings and that two separated leading edge vortices, inboard and outboard, can be formed over a double-delta wing surface. The two vortices are separated from each other at small angles of attack, and the inboard vortex merges with the outboard one when the angles of attack are increased. The numerical results are in good agreement with Hummel's experiments.[9] According to the rolled-up leading-edge vortices and Donaldson's criterion,[14] the numbers, positions, and signs and strength of rolled up trailing-edge vortices may be predicted. A simplified method that may improve the predicting of downwash field is suggested.

I. Introduction

In recent years there has been a growing interest in rolling up of leading-edge vortex sheets of wings. The flow is separated along the leading edge of a slender wing forming a free shear layer, while rolling up to form a spiral-shaped vortex core on each side of the wing. These leading-edge separated vortices induce additional nonlinear lift on the wing, often is the called vortex-induced lift. The complicated interactions between vortex/vortex and vortex/surface are particularly important for accurately predicting aerodynamic characteristics on aircraft and missile.

The investigation of the leading-edge separated vortex began as early as in the 1940's and 1950's. In the early stage, theoretical models used were based on the conic flow assumption, made by Mangler and Smith[1] and improved by Smith.[2] Later, Belotserkovski[3] and Kandil et al.[4] developed a vortex lattice method with an edge-separated vortex that was replaced by a number of discrete-line vortices. To accurately calculate the pressure distribution on wings, Johnson et al.[5] presented a three-dimensional free vortex sheet model, using a higher-order panel method. Hoejimakers et al.[6,7] reported their experimental and theoretical results for delta-like wings and developed a second order panel method to calculate double-branched spiral vortices. A wide review of the subject has been made by Smith.[8]

We are very interested in is a series of experiments conducted by Hummel et al.[9,10] They measured the spatial flowfield in detail and plotted the contours of total pressure, dynamic pressure, and flow directions above the wing surface and downstream. These experimental results have led us to a better understanding of the feature regarding the formation of leading-edge and trailing-edge vortices and their interactions. A scheme of the flow pattern is shown in Fig. 1.

In the present paper we implemented a discrete vortex model, in the slender-body framework, to simulate the rolling up of vortex sheets on delta and double-delta wings. The discrete-vortex model has applied widely to simulate the evolution of vortex sheet. The particular advantage of the discrete-vortex method is its simplicity and flexibility. Unfortunately, these discrete vortices have the tendency of random motion. Some authors have suggested several smoothing techniques, such as vorticity redistribution, vortex amalgamation, viscous vortex core, etc., or a combination of these techniques, which attempt to mitigate the random motion. Furthermore, another serious shortcoming arising from the slender-body framework is that the flow cannot match the Kutta condition at trailing edge. Therefore, no matter which smoothing technique is applied, the surface pressure distribution in chord direction can not be calculated accurately.

The main aim of this paper is to investigate the rolling up of complicated vortex sheets and the effect of the interaction of those vortex sheets on the downwash field rather than to examine smoothing schemes. We will also discuss how the prediction of the aerodynamic characteristics of downwash field can be improved according to the feature of rolling up of vortex sheets.

II. Theoretical Analysis

To study the interaction between leading- and trailing-edge vortices, we must first calculate the rolling up of the leading-edge vortex over the wing surface and also obtain the vorticity strength distribution; i.e., we have to obtain the spanwise circulation distribution on the wing at the trailing edge. Figures 2 and 3 show the pressure distribution and the vortex lines on the surface measured by Hummel.[9] One can see from these figures that the surface pressure distribution and the vortex lines are essentially different from those obtained according to the linearized slender wing theory of Jones[15] because of the presence of the leading-edge vortex. However, they are qualitatively similar to those obtained by Smith's model.[2] We con-

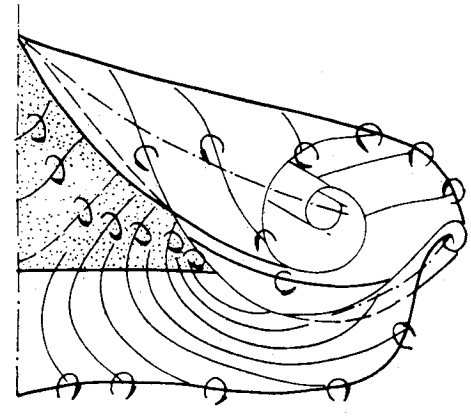

Fig. 1 Schematic diagram for the formation of downstream vortices of a slender delta wing.

Received May 11, 1987; revision received Aug. 15, 1988.

*Associate Professor.

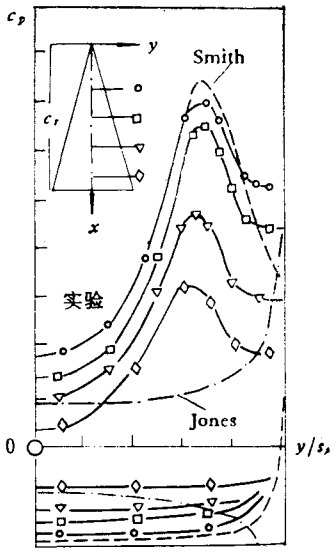

Fig. 2 Pressure distribution on delta wing: $\Lambda = 1.0$, $\alpha = 20.5$ deg.

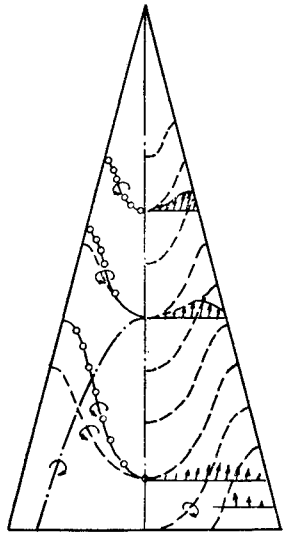

Fig. 3 Bound vortex vector (R) and bound vortex lines (L).

sider, as the results of preliminary studies show, that a two-dimensional model in the slender-body theory can reflect the major features of the flow.

A three-dimensional steady flow around a slender wing with an angle of attack can be analyzed approximately by a two-dimensional time-dependent flow analogy in a crossflow plane. The separated free shear layer emanating from the leading edge of the wing is replaced by a finite number of two-dimensional point vortices. This model does not limit the assumption of conical flow, which can be used to compute the rolling up of several concentrated vortices for a complicated wing configuration. Therefore, the velocity potential φ of the flow satisfies the Laplace equation in a crossflow plane

$$\frac{\partial^2\varphi}{\partial y^2} + \frac{\partial^2\varphi}{\partial z^2} = 0$$

It is convenient to use a complex function method. The wing section in the crossflow plane, $X = y + iz$, can be transformed into a circle in the transformed plane, $\zeta = \xi + i\eta$ by use of conformal mapping. Hence, the resulting problem is reduced to a flow around a circle with a finite number of point vortices outside the circle. The complex potential of the flow is

$$W(\zeta) = -\frac{i}{2}|V_\infty| \sin\alpha\left(\zeta - \frac{s^2}{\zeta}\right) - \sum_{j=1}^{N} \frac{i\Gamma_j}{2\pi} \ln \frac{[\zeta - \zeta_j][\zeta + (s^2/\zeta_j)]}{[\zeta - \bar{\zeta}_j][\zeta - (s^2/\bar{\zeta}_j)]} \tag{1}$$

For flat-plate wing the conformal mapping is the Joukowski transformation $X = \frac{1}{2}[\zeta + (s^2/\zeta)]$ [or $\zeta = X + (X - s^2)^{1/2}$], where s is the half-width of the plate. The Kutta condition must be satisfied at leading edge of the wing; thus, we get

$$\sum_{j=1}^{N} \frac{\Gamma_j}{2\pi}\left\{\frac{\zeta_j}{\zeta_j^2 - s^2} + \frac{\bar{\zeta}_j}{\bar{\zeta}_j^2 - s^2}\right\} = \tfrac{1}{2}|V_\infty| \sin\alpha \tag{2}$$

The point vortices move downstream at the local velocities. The velocity of the kth vortex is expressed as

$$v_k - iw_k = (G_1 + G_2 + G_3)\left.\frac{d\zeta}{dX}\right|_{X_k} + G_4 \tag{3}$$

where

$$G_1 = -\frac{i}{2}|V_\infty| \sin\alpha\left(1 + \frac{s^2}{\zeta_k^2}\right)$$

$$G_2 = -\sum_{j\neq k}^{N} \frac{i\Gamma_j}{2\pi} \frac{1}{\zeta_k - \zeta_j}$$

$$G_3 = -\sum_{j=1}^{N} \frac{i\Gamma_j}{2\pi}\left[\frac{1}{\zeta_k + (s^2/\zeta_j)} - \frac{1}{\zeta_k + \bar{\zeta}_j} - \frac{1}{\zeta_k - (s^2/\bar{\zeta}_j)}\right]$$

$$G_4 = -\frac{i\Gamma_k}{2\pi} \frac{s^2}{\zeta_k^3[1 - (s^2/\zeta_k^2)]}$$

$$\left.\frac{d\zeta}{dX}\right|_{X_k} = -\frac{2}{1 - (s^2/\zeta_k)}$$

Strength and Position of Nascent Vortex

In two-dimensional unsteady flow analogy, each point vortex represents the vorticity shed from the leading edge during a time interval. The number of point vortices N is to increase in the flowfield with time. There are effects of the strength of the nascent vortex on the shape of the rolling up of the leading-edge vortex and on the surface pressure distribution. Many authors have investigated this problem. Sacks et al.[11] used two methods, either theoretical or empirical, to calculate the strength of the nascent vortex. Here, we also use two methods. The first one is similar to Sacks' theoretical one. The variation of the circulation of shear layer with time near the leading-edge separated point is

$$\frac{\partial\Gamma}{\partial t} = \tfrac{1}{2}(V_{\text{low}}^2 - V_{\text{up}}^2) \tag{4}$$

where V_{up} and V_{low} represent the velocities at the upper and lower surface of shear layer, respectively. We let $V_s = \frac{1}{2}(V_{\text{up}} + V_{\text{low}})$, the average velocity of the shear layer, which represents the velocity at which the shear layer is shed from the leading edge. The equation $\gamma_x = V_{\text{low}} - V_{\text{up}}$ is vorticity strength on a unit length of the shear layer. Therefore, Eq. (4) can be rewritten as

$$\Delta\Gamma_{\text{new}} = \Delta t(V_s\gamma_x) = (V_s\Delta t)\cdot\gamma_x = \Delta s\cdot\gamma_x \tag{5}$$

where Δs is the length of the shear layer shed out in Δt time. The expression for V_s is found to be

$$v - iw|_s = \sum_{j=1}^{N} \frac{is\Gamma_j}{2\pi}\left[\frac{\zeta_j^2}{(\zeta_j^2 - s^2)^2} - \frac{\bar{\zeta}_j^2}{(\bar{\zeta}_j^2 - s^2)^2}\right] \tag{6}$$

In fact, w_s is equal to zero due to flow symmetry. There is only a y-direction velocity component, which implies that the shear layer is shed out tangentially from the leading edge. In our computation, V_s is computed with Eq. (6) so that the length Δs can be determined. Then, the nascent point vortex is placed at the half-length of the vortex layer increment, $0.5\Delta s$. The strength of the nascent vortex is obtained by using the Kutta condition [Eq. (2)].

In the second method the vortex strength can be determined by using the leading-edge suction analogy as well as a vortex-impulse theorem. Initially, the suction analogy theory by Polhamus could only calculate the overall vortex-induced lift. Later, Purvis[12] suggested an analytical method that could be used to calculate the distribution of the suction along the leading edge. Then the vortex-induced lift of the front part of the axial station x_i is given by

$$CL_{vle} = E_1 C_k \int_0^{\eta} (\eta_1\sqrt{1-\eta_1^2} + \sin^{-1}\eta_1)/\cos\Lambda \, d\eta_1 \qquad (7)$$

The meaning of the formula can be seen from Ref. 12. On the other hand, according to the vortex-impulse theorem, the vortex-induced lift is also equal to

$$CL_{vle} = \frac{4\pi}{S_w}\sum_{j=1}^{N-1}\frac{\Gamma_j}{2\pi V_\infty} Re\left\{\zeta_j - \frac{s^2}{\zeta_j}\right\} + \frac{4\pi}{S_w}\frac{\Gamma_n}{2\pi V_\infty}\left(\xi_n - \frac{s^2}{\xi_n}\right) \qquad (8)$$

where Γ_n and ξ_n are nascent vortex strength and position, respectively. Moreover, the Kutta condition [Eq. (2)] must be satisfied at each axial station. From Eqs. (7), (8), and (2) the nascent vortex strength and position can be determined.

Surface Pressure Distribution and Bound Vortex Lines

From the definition of the pressure coefficient, we get

$$C_P = \sin^2\alpha - \frac{2\varphi_x}{V_\infty}\cos\alpha - \frac{\varphi_x^2 + \varphi_y^2 + \varphi_z^2}{V_\infty^2} \qquad (9)$$

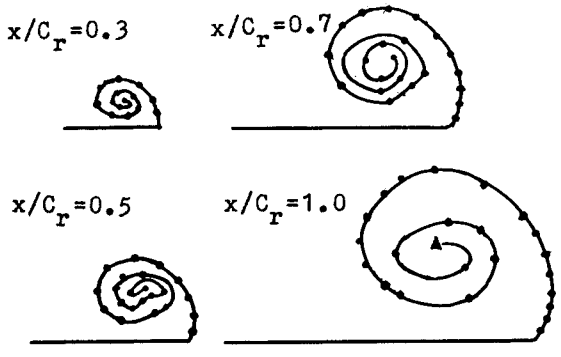

Fig. 4 Rolling up of leading-edge vortex over delta wing.

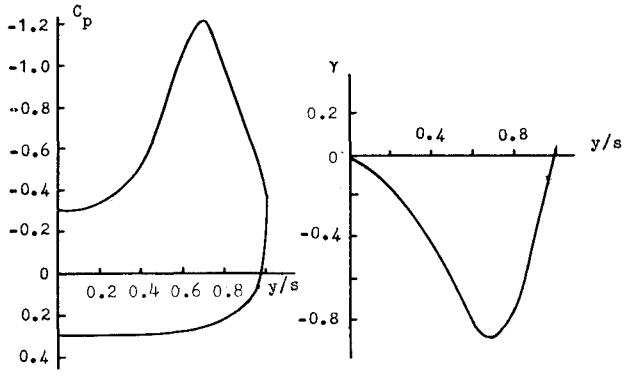

Fig. 5 Surface pressure and bound vortex distribution at trailing edge of wing.

where $\varphi_x = u$, $\varphi_y = v$, and $\varphi_z = w$, and u, v, and w are velocity components in the x, y, and z directions, respectively. The calculation of φ_x must take accounts of two aspects. One is that the semi-wing span $s(x)$ is a function of x. The variation caused by $s(x)$ is

$$\varphi_x = \frac{ds(x)}{dx} \cdot R.P. \frac{\partial W(X)}{\partial s}$$

The other is caused by the variation of the point vortices with x. The derivation of the entire formula is tedious. It is omitted here. The bound vortex lines on the wing surface can be evaluated by

$$\gamma = \gamma_x \boldsymbol{i} + \gamma_y \boldsymbol{j} = -(v_{up} - v_{low})\boldsymbol{i} + (u_{up} - u_{low})\boldsymbol{j} \qquad (10)$$

where the γ is vorticity vector, and the subscripts up and low represent the upper and lower surface, respectively. Because $\gamma_x = -(\partial\Gamma/\partial y)$, the strength of the ith trailing edge vortex is

$$(\Delta\Gamma_i)_{trail} = \int_{y_i}^{y_{i+1}} (\gamma_x)_{trail} \, dy \qquad (11)$$

III. Numerical Results

Mathematically, this calculation is to solve first-order ordinary differential equations, using the Runge-Kutta method. However, it should be noted that the number of point vortices N is variable from the apex of the wing to the trailing edge. A new vortex shed from the leading edge is introduced into the

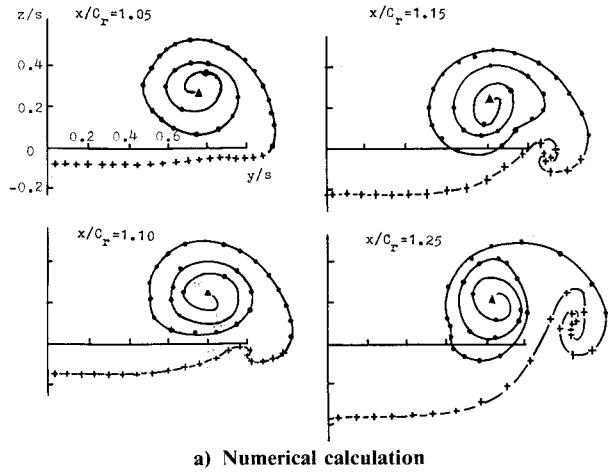

a) Numerical calculation

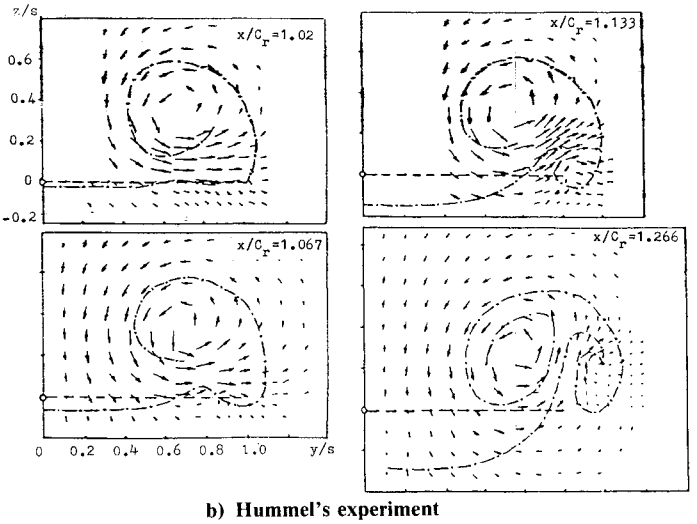

b) Hummel's experiment

Fig. 6 Evolution of rolling up of leading and trailing vortices and their interaction.

flowfield at each axial station x_i. Downstream from the trailing edge, the trailing-edge vortex sheet must be considered along with the leading-edge vortex sheet. If the leading/trailing-edge vortex sheets are replaced by N_l and N_t point vortices, respectively, the evolution of the trailing-edge vortex sheets under the influence of the leading-edge vortex sheet can be simulated by computing the motion of those vortices from the trailing-edge step by step downstream.

Delta Wing

As an example, we calculated a delta wing with an aspect ratio $\Lambda = 1.0$ and an angle of attack $\alpha = 20.5$ deg. Figure 4 shows the rolling up of the leading-edge vortex over the wing surface. Figure 5 shows the pressure distribution and bound vorticity strength distribution at the trailing edge. The pressure distribution is close to Smith's.[2]

Figure 6a shows the rolling up of leading/trailing-edge vortices and their interaction. From those figures one can see that these vortices are quite similar go those obtained by Hummel[9] (see Fig. 6b). One can also see from Fig. 6a that the trailing-edge vortex sheet already arises to deformation at the place $x/C_r = 1.05$, close to the trailing edge downstream, where C_r is the length of root chord of the wing. Following downstream, the deformation continues to enlarge and gradually rolls up into a clockwise concentrated vortex under the influence of the leading-edge vortex. At the same time, the trailing edge vortex sheet has been stretched. The trailing-edge vortex is initially on the right lower side of the leading-edge vortex; then, it moves outward and gradually rises around the leading-edge vortex. The trailing concentrated vortex has developed well at approximately one-fourth of a wing span of trailing edge downstream. The circulation of the trailing vortex is of opposite sign to that of the leading-edge vortex.

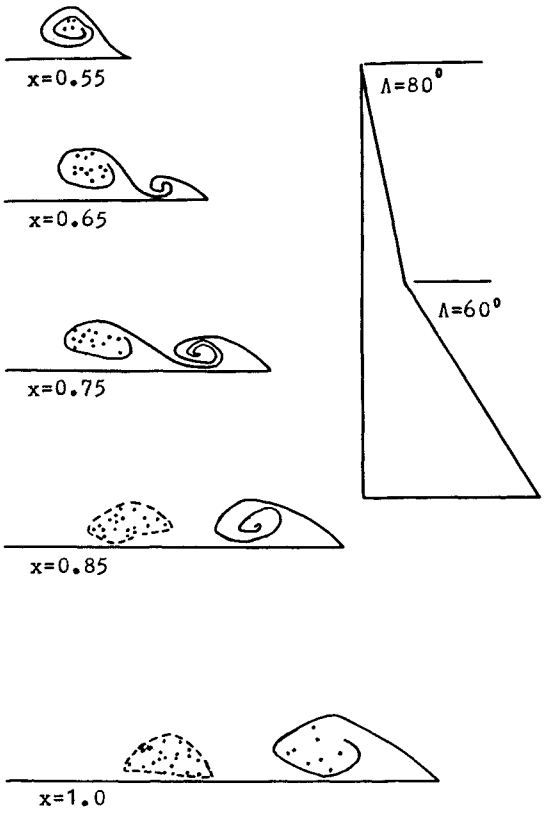

Fig. 7 Evolution of the inboard wing vortex sheet at $\alpha = 12$ deg for Hummel's no. VI model.

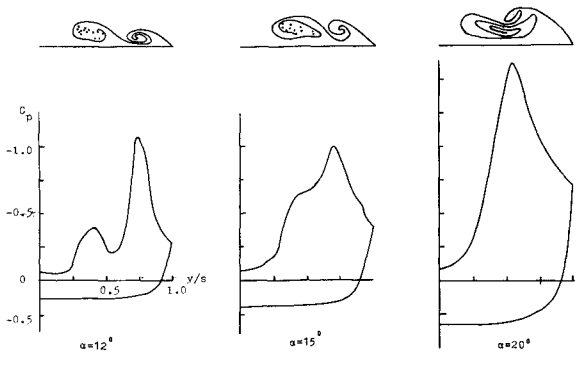

Fig. 8 Flow pattern and surface pressure distribution at $x = 0.7$.

Double Delta Wing

The numerical example for double-delta wing, i.e., Hummel's No. VI model, which in Fig. 7 shows geometrically, has been computed. The calculated results show that the inboard vortex sheet shed from the fore part of the leading edge upstream of the kink, and the outboard vortex sheet shed from just downstream of the kink may form two separated concentrated vortices with the same direction of rotation. Figure 7 shows the evolution of vortex sheets at the following positions downstream of the kink. Downstream of the leading-edge kink, the inboard vortex is no longer increasing its strength with vorticity, but the outboard vortex continues to enhance from the fed vorticity from the leading edge. The inboard vortex sheet rolls up well up to $x = 0.75$, after which these point vortices become very disorderly. However, they are still form a group of vortex clouds that represent the inboard vortex.

Figure 8 shows the calculated flow pattern and surface pressure distribution at $x = 0.7$, where $\alpha = 12$, 15, and 20 deg. At $\alpha = 12$ deg, the inboard and outboard vortices are separated, and there are two suction peaks on the upper surface beneath the strake and wing vortex cores, respectively. Although at $\alpha = 15$ deg the two concentrated vortices remain distinguishable, the inboard vortex moves outward, close to the outboard vortex, showing only one suction peak. The inboard suction peak becomes a small protrusion on the pressure curve. At $\alpha = 20$ deg, the inboard vortex moves under the outboard vortex and becomes distorted. The shape of pressure curve is the same as that formed by one wing vortex. Generally, the inboard and outboard vortices are separated from each other up to the trailing edge for small angles of attack, approximately lower than 12 deg. The inboard vortex merges with the outboard vortex at the trailing edge at $\alpha > 12$ deg. The position of merged point will move upstream with an increased angle of attack. The coalesced process is related to their relative strength and position of the two vortices; however, it is not clear what the coalesced condition is.

Figure 9 shows the formation of the trailing-edge concentrated vortex. The circulation of the trailing-edge vortex is of

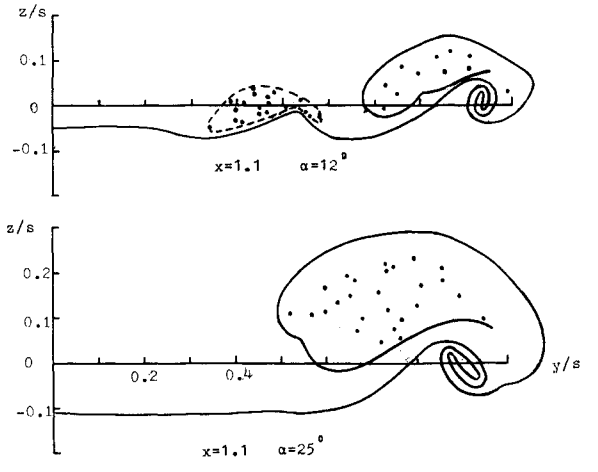

Fig. 9 Formation of trailing-edge vortex.

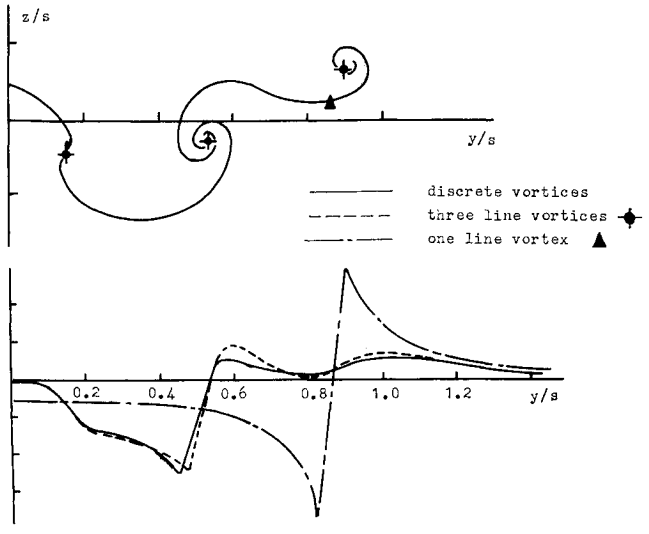

a) Rolling Up of a Complicated Vortex Sheet and Downwash Velocity

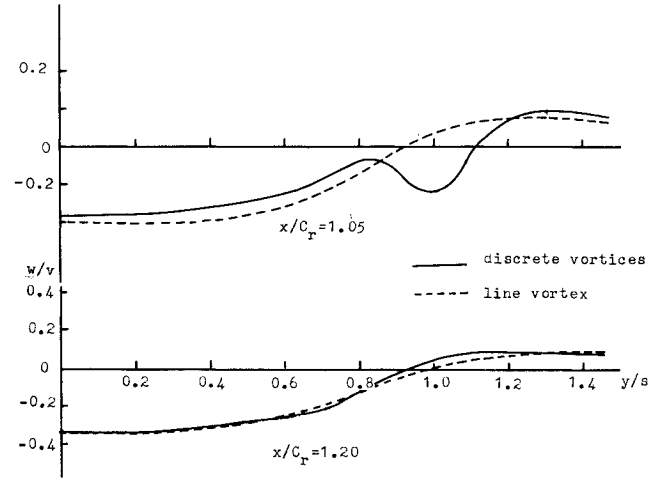

b) For Delta Wing $\Lambda = 1.0$ $\alpha = 20.5°$

Fig. 10 Downwash velocity distribution.

opposite sign to that of the leading-edge vortices, and the concentrated trailing-edge vortex will move outward and upward around the leading-edge vortices. Because the inboard wing vortex is weak, it can deform the trailing-edge vortex sheet only slightly and not form another concentrated vortex (see Fig. 9a). In Fig. 9b, there exists one wing vortex and one trailing-edge vortex, similar to that produced by delta wing (see Fig. 6). The inboard vortex has been merged here.

IV. Discussion of Downwash Field

The effect of downwash field induced by the fore wing on the rear wing is important for predicting force and moment imposed on aircraft or missiles. In the case of attached flow at a small angle of attack, the downwash field is usually divided into a "near field," in which the trailing vortex sheet is considered as a flat vortex sheet, and a "far field," in which the vortex sheet is replaced by a line vortex. But, in the case of flow with leading-edge separated vortices at moderate to high angles of attack, how can the characteristics of the downwash field be predicted? There is a method used in engineering design in which the normal lift is divided into potential flow lift and vortex-induced lift; thus $C_{N_{tot}} = C_{N_{w,p}} + C_{N_{w,v}}$. Then, the strength of trailing- and leading-edge vortices of the fore wing can be determined:

$$\left(\frac{\Gamma}{V_\infty}\right)_t = \frac{S}{4y_t} C_{N_{w,p}} \cos\alpha \tag{12a}$$

$$\left(\frac{\Gamma}{V_\infty}\right)_v = \frac{S}{4y_v} C_{N_{w,v}} \cos\alpha \tag{12b}$$

where subscripts t, v, and p represent trailing-edge vortex, leading-edge vortex, and potential flows, respectively, and S is wing area. The span position of the trailing-edge vortex y_t is determined according to the span circulation distribution at the trailing edge of the wing, and the perpendicular position z_t is zero. The positions of the leading-edge vortices y_v and z_v are given by empirical curves. However, as mentioned earlier, the span circular distribution of bound vortex at the trailing edge calculated by attached flow theory without leading-edge vortex is substantially different from that with leading-edge separated vortices. At least, for delta-like wings shown by Hummel's experiments and present numerical results, there can exist one-core or multicore leading-edge vortices; hence the trailing vortex sheet can also be rolled up one-core or multicore vortices with opposite sign to leading-edge vortices. One must be careful that Eq. (12a) is used to calculate the bound vortex circulation Γ, particularly when there are complicated leading-edge vortex sheets.

Figure 10 shows the downwash velocity distribution at an across plane in body coordinate system. Figure 10a shows the rolling up of a trailing vortex sheet with a complicated circulation distribution.[13] It formed three vortex cores: the inboard one is called the "fuselage" vortex, the outboard is the "tip" vortex, and the middle is the "flap" vortex. If the vortex sheet is replaced by three-line vortices, the computed downwash velocity (dashed line) is very close to that by the discrete-vortex model (real line), but is quite different from that by the one-line vortex (dot line).

Figure 10b shows the downwash velocity distribution at two various axial position for the delta wing: $\Lambda = 1.0$ and $\alpha = 20.5$ deg The real line shows the results using discrete-vortices model. The detached lines shows the results that the vortex sheets have been replaced by a one-line vortex. Both hardly have any difference when $x/cr \geq 1.20$. A fair result can be obtained even using one concentrated vortex. It is because the leading edge vortex has rolled up quite well already at trailing edge, and the trailing-edge vortex is quite weak. It is possible that a simplified model can be presented according to the practical shape rolled vortices.

Donaldson et al.[14] has proposed a criterion that can estimate the numbers, positions, and circulation signs of the concentrated vortices rolled up from an initial vortex sheet. It is stated that the vortices will be rolled up near those parts of the maximum absolute values of vorticity in an initial vortex sheet.

We find that it is useful to use the criterion of Donaldson et al.[14] when computing complicated downwash field. A simplified engineering model of downwash field may be included with the following aspects:

1) Determine the numbers, strength, and position of vortices rolled up from leading-edge vortex sheet using either the empirical or the theoretical method.

2) Determine the span circulation distribution of the wing surface at the trailing edge under the influence of leading-edge vortices.

3) According to the criterion of Donaldson et al.,[14] estimate the numbers, positions, and sign and strength of vortices rolled by the trailing-edge vortex sheet.

4) These rolled vortices are simplified into several line vortices and their motion and downwash field are calculated.

V. Conclusion

In the present paper we compute the rolling up of leading/trailing-edge vortex sheets and their interaction for delta and

double-delta wings. We show that a particular advantage of the discrete-vortex method is its simplicity and flexibility, which can be used to compute the rolling up of multicore vortices for a complicated wing configuration. The numerical results show that a trailing concentrated vortex that has an opposite sign of circulation of leading edge vortex sheets can be formed under the influence of leading-edge vortex sheets, at least for delta-like wings, and also that the two separated vortices, inboard and outboard, may be rolled up over a double-delta-wing surface. Generally, the two vortices are separated from each other at small angles of attack. When the angles of attack are increased, the inboard vortex may move, close to, and finally merge with the outboard one. The numerical results are in good agreement with Hummel's experiments.[9] According to the rolled-up leading-edge vortices and the criterion of Donaldson et al.[14] the numbers, positions, and signs and strength of rolled-up trailing-edge vortices can be predicted. Therefore, an improved method is suggested that can predict downwash field.

References

[1]Mangler, K. W. and Smith, J. H. B., "A Theory of the Flow Past a Slender Delta Wing with Leading-Edge Separation," *Proceedings of the Royal Society of London, Series A,* Vol. 251, 1959, pp. 200–217.

[2]Smith, J. H. B., "Improved Calculations of Leading-Edge Separation from Slender, Thin, Delta Wing," *Proceedings of the Royal Society of London, Series A,* Vol. 306, 1968, pp. 67–90.

[3]Belotserkovski, S. M., "Calculation of the Flow around Wings of Arbitrary Planforms in a Wide Range of Angles of Attack," NASA TT F-12, 291, May 1969.

[4]Kandil, O. A., Mook, D. T., and Nayfeh, A. H., "Nonlinear Prediction of Aerodynamic Loads on Lifting Surface," *Journal of Aircraft,* Vol. 13, Jan. 1976, pp. 22–28.

[5]Johnson, F. T., Johnson, F. J., Lu, P., Brune, G. W., Weber, J. A., and Rubbert, P. E., "An Improved Method for the Prediction of Completely Three-dimensional Aerodynamic Load Distributions of Configurations with Leading-Edge Vortex Separation," AIAA Paper 76-417, 1976.

[6]Hoejimakers, H. W. M. and Vaatstra, W. "A Higher-Order Panel Method Applied to Vortex Sheet Roll-Up," *AIAA Journal,* Vol. 21, April 1983, pp. 516–523.

[7]Hoejimakers, H. W. M., Vaatstra, W., and Verhaagen, N. G., "Vortex Flow Over Delta and Double-Delta Wings," *Journal of Aircraft,* Vol. 20, Sept. 1983, pp. 825–832.

[8]Smith, J. H. B., "Theoretical Modeling of Three-Dimensional Vortex Flows in Aerodynamics," *Aeronautical Journal,* Vol. 88, April 1984, p. 101.

[9]Hummel, D., "On Vortex Formation over A Slender Wing at Large Angles of Incidence," AGARD CP-247, Jan. 1976.

[10]Brennestuhl, U. and Hummel, D., "Untersuchungen über die Wirbelbildung an Flugen mit Geknickten Vorderkanten," Zeitschrift für Flugwissenschaften und Weltraumforschung, Vol. 5, 1981, pp. 375–381.

[11]Sacks, A. H., Sacks, A. H., Lundberg, R. E., and Hanson, C. W., "A Theoretical Investigation of Slender Wing Body Combinations Exhibiting Leading Edge Separation," NASA CR-719, March 1967.

[12]Purvis. J. W., "Analytical Prediction of Vortex Lift," *Journal of Aircraft,* Vol. 18, April 1981, pp. 225–230.

[13]Baker, G. R., "The 'Cloud in Cell' Technique Applied to the Roll Up of Vortex Sheets," *Journal of Computational Physics,* Vol. 31, April 1979, pp. 79–95.

[14]Donaldson, C. D., Snedeker, R. S., and Sullivan, R. D., "Calculation of Aircraft Wake Velocity Profiles and Comparison with Experimental Measurements," *Journal of Aircraft,* Vol. 11, 1974, pp. 547–555.

[15]Jones, R. T., "Properties of Low Aspect Ratio Pointed Wings at Speeds Above and Below the Speed of Sound," NACA Rept. 835, 1946.

[16]Polhamus, E. C., "A Concept of the Vortex Lift of Sharp-Edge Delta Wing Based on a Leading-Edge Suction Analogy," NASA TN-D-3767, 1966.